Macromolecular Research, Vol. 17, No. 11, pp 931-933 (2009)

Notes

Miniemulsion Polymerization of Styrene in the Presence of Graphite Nanosheets

Jeongwoo Lee, Jinho Hong, and Sang Eun Shim*

Department of Chemical Engineering, Inha University, Incheon 420-751, Korea

Dongsoo Jung

Department of Mechanical Engineering, Inha University, Incheon 420-751, Korea

Received January 2, 2009; Revised April 20, 2009; Accepted April 20, 2009

Introduction

Graphite nanosheets are composed of a honeycomb arrangement of carbon atoms and are the basis of carbon nanotubes.[1] They have received much attention as a viable filler in composite materials because they offer high thermal and chemical stability and improved electrical conductivity. Therefore, the composites can be a good candidate in electromagnetic interference (EMI) shielding, radar evasion, rechargeable batteries, conductive inks, and antistatic textiles.[2-4] However the graphite nanosheets have the strong van der Waals force, resulting in self-aggregation. Such character interrupts a fine dispersion of graphite nanosheets in matrix materials. To overcome such obstacles, a number of research has dealt with surface modification of graphite nanosheets. Therefore, graphite nanosheets/polymer composites have been produced by *in situ* polymerization such as solution,[5] suspension,[6] emulsion,[7] and bulk polymerizations.[8]

The miniemulsion polymerization method has merits over other techniques because it produces smaller size-polymer particles.[9] Therefore, in several papers, the carbon material/polymer composite materials have been prepared by miniemulsion polymerization[9,10] and we have explored a simple and fast method to produce the graphite nanosheet/polystyrene (PS) composites using miniemulsion polymerization. These graphite nanosheet/PS composites can be incorporated successfully into polymer matrix by mechanically mixing or static melt dispersion mixing as a conductive filler.

*Corresponding Author. E-mail: seshim@inha.ac.kr

Experimental

Graphite nanosheets with an average size of 5 μm were supplied by N-Baro Tech (Ulsan, Korea) and used without further purification. Dodecyl sulfate sodium salt (SDS, 85%) was supplied by Acros Organics, Belgium and was used as a stabilizer. Styrene (extra pure, Junsei, Japan) was used as received and stored at -5 °C prior to use. 2,2-Azobis(isobutyronitrile) (AIBN, Junsei) was used as a initiator without further purification. Hexadecane (Aldrich Co., USA) was used as a co-stabilizer.

The graphite nanosheet/PS composites were produced via the following procedure. Graphite nanosheets (0.05, 0.07, 0.1, 0.12, and 0.15 g) were dispersed with SDS (0.5 g) and hexadecane (0.3 g) in 200 mL of deionized water and then ultrasonicated for 30 min (200 W, Sonics Co., USA). Styrene (2 g) and AIBN (0.02 g) were mixed before polymerization. The solution dispersed graphite nanosheets with SDS and hexadecane, and the mixture of styrene and AIBN were transferred into 500 mL three-necked round bottom flask and then ultrasonicated at 0 °C for 10 min (200 W). The reactor temperature was raised to 60 °C in oil bath with mechanical stirring at 500 rpm under nitrogen atmosphere for 24 h. On the other hand, the concentration of graphite nanosheets was fixed at 5.0 wt%, while the divinylbenzene (DVB, Aldrich Co., USA) was changed to check out the effect of cross-linkage. This experiment was carried out in the same process except for simultaneous use of styrene (1.8 g) and DVB (0.2 g). After completion of the polymerization, the resultants were rinsed off with deionized water and methanol, then centrifuged repeatedly to remove the residual styrene and SDS.

The morphologies of the graphite nanosheet/PS composite particles were characterized by scanning electron microscopy (SEM, S-4300, Hitachi) and transmission electron microscopy (TEM, CM200, Philips). The dispersion stability of the composites in toluene was monitored by measuring the transmission of monochromatic light (λ=880 nm) from the suspension employing an optical analyzer, Turbiscan LAB (Formulaction, France). The electrical conductivities of the pure PS and composite film were measured by a resistivity meter (Loresta-GP, Misubishi Chemical Co., Ltd. Japan).

Results and Discussion

The morphology of graphite nanosheet/PS composites with different concentrations of graphite nanosheets is shown in Figure 1. It is seen that the PS particles are produced at only specific concentration of graphite nanosheets (Figure 1(c),(d)). We can consider that the formation of monomer-swollen SDS micelles is influenced by the concentration of graphite

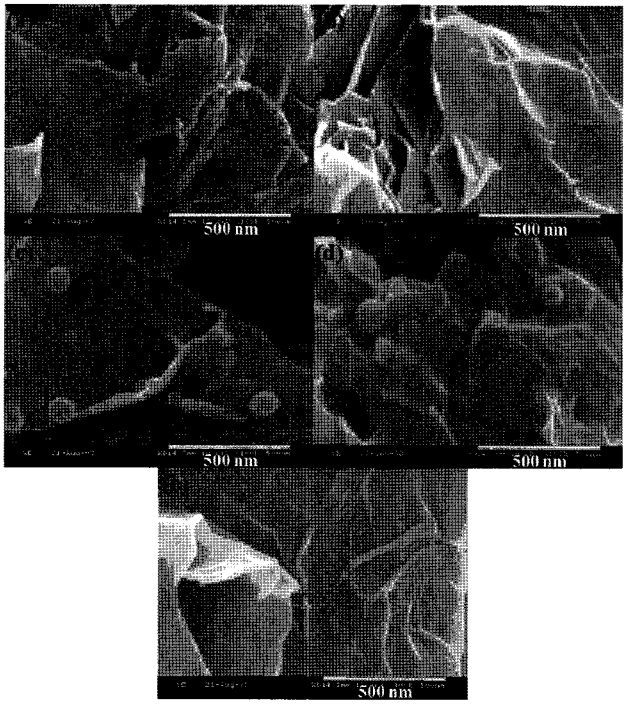

Figure 1. SEM photographs of graphite nanosheets/PS composites with different concentrations of graphite nanosheets: (a) 2.5, (b) 3.5, (c) 5.0, (d) 6.0, and (e) 7.5 wt% relative to styrene.

nanosheets. The SDS surface micelles containing styrene attach to graphite nanosheet surfaces because of the chemical affinity.[9] At 2.5 wt% graphite nanosheets relative to styrene, the graphite nanosheets are covered with SDS (Scheme I(a), Figure 1(a)). Since the concentration of SDS is too much than other samples, SDS is packed close together. Therefore, micelles cannot be produced on graphite nanosheet surfaces and PS thin film is produced. But at 5 wt% graphite nanosheets, SDS is arranged wider than at 2.5 wt% (Scheme I(b), Figure 1(c)). Therefore, micelles are produced on graphite nanosheet surfaces and PS particles are resulted. Finally, at 7.5 wt%, SDS is not enough to produce micelles (Scheme I(c), Figure 1(e)).

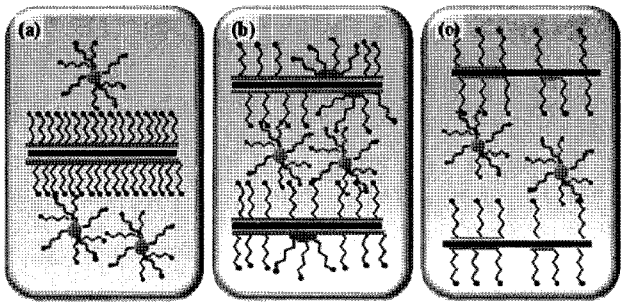

Scheme I. Three different arrangement of SDS on graphite nanosheet surfaces: (a) 2.5, (b) 5.0, and (c) 7.5 wt% graphite nanosheets relative to styrene.

Therefore, there are PS thin films spatially distributed on the graphite nanosheets. The morphology of composites at 3.5 wt% (between 2.5 and 5.0 wt%) and 6.0 wt% (between 5.0 and 7.5 wt%) was investigated to ascertain our estimation. As the PS thin film is produced at 3.5 wt% (Figure 1(b)) and the PS particles are produced at 6.0 wt% (Figure 1(d)), the two composites satisfy the assumption. Figure 2 represents the TEM micrographs of graphite nanosheet/PS composites at 2.5, 5.0, and 7.5 wt% graphite nanosheets relative to styrene. These TEM micrographs show that the expectation is correct. Although the PS thin film is not exactly distinguished by SEM micrograph, we can confirm the existence in Figure 2(a). In addition, we can observe PS particles in Figure 2(b) and the rare PS thin film in Figure 2(c).

Since we confirmed that PS particles were successfully synthesized on surface of graphite nanosheets at 5.0 wt% graphite nanosheets (Figure 1(c)), the concentration of graphite nanosheets was fixed at 5.0 wt%, while DVB was incorporated to explore the effect of cross-linkage. The SEM micrographs of the resultants are shown in Figure 3. There are more PS particles on the graphite nanosheets surface when DVB was used (Figure 3(b)), compared to the case without DVB (Figure 3(a)). It has been found that some degree of styrene was absorbed as graphite nanosheets have a good affinity for styrene.[10,11] It is worthy to mention that the PS particles are so strongly bound with the graphite

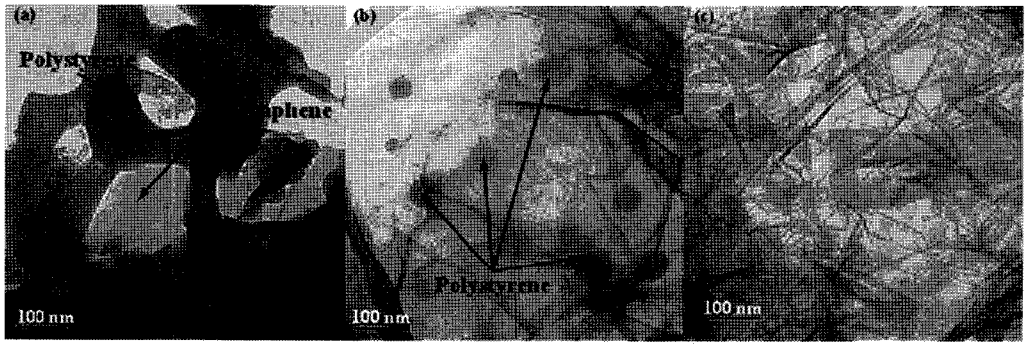

Figure 2. TEM micrographs of graphite nanosheets/PS composites with different concentrations of graphite nanosheets: (a) 2.5, (b) 5.0, and (c) 7.5 wt% relative to styrene.

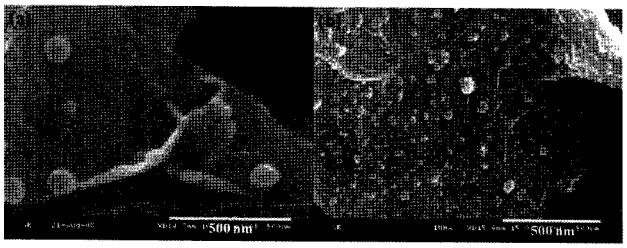

Figure 3. SEM micrographs of graphite nanosheets/PS composites produced (a) without DVB and (b) with DVB.

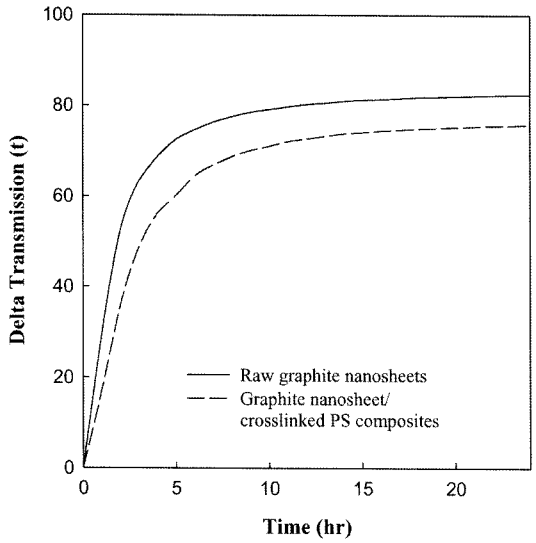

Figure 4. Dispersion stability of 0.001 wt% raw graphite nanosheets and graphite nanosheet/crosslinked PS composites dispersed in toluene.

nanosheets that we could not detach the particles even by powerful ultrasonication for 30 min (200 W). Therefore, it represents that PS particles are strongly bound to the surface of graphite nanosheets because of the crosslinking reaction.

Figure 4 depicts the dispersion stability of 0.001 wt% raw and crosslinked PS composited graphite nanosheets in toluene monitored for 24 h. This dispersion stability would provide with an insight that the raw graphite nanosheets form much more an aggregated structure than the composites. Therefore, the delta transmittance of raw graphite nanosheets shows a faster increase with time than that of the composites. Therefore, these graphite nanosheet/crosslinked PS composites can be incorporated successfully into polymer matrix by mechanically mixing or static melt dispersion mixing as a conductive filler.

The electrical conductivities of graphite nanosheet/PS composite film are shown in Table I. The emulsion polymerized graphite nanosheet was solution-casted with virgin PS with a fixed concentration of graphite nanosheet, 10 wt%. It is seen that the electrical conductivity increased with the addition of the graphite nanosheet.

Table I. The Electrical Conductivity of Pure PS and Graphite Nanosheet/PS Composite Film

	Pure PS Film	10 wt% Graphite Nanosheet/PS Composite Film
Electrical Conductivity	1×10^{-16} S/cm	8.05×10^{-5} S/cm

Conclusions

Miniemulsion polymerization of styrene was performed in the presence of carbon nanosheets. As a result, PS particles were introduced onto the surface of graphite nanosheets by the miniemulsion polymerization. The formation of SDS surface micelles is influenced by the concentration of graphite nanosheets. Therefore, the composites show three different surface morphologies of graphite nanosheets surfaces; (1) the surface attached with PS particles, (2) the surface covered with PS thin film, and (3) the bare exposed surface. The crosslinked PS particles strongly stick to the surface of graphite nanosheets and the graphite nanosheet/crosslinked PS composites show much improved dispersion stability in toluene.

Acknowledgments. This work was supported by the Korea Science and Engineering Foundation (grant no. R01-2007-000-20055-0).

References

(1) M. J. McAllister, J. L. Li, D. H. Adamson, H. C. Schniepp, A. A. Abdala, J. Liu, M. Herrera-Alonso, D. L. Milius, R. Car, R. K. Prud'homme, and I. A. Akasay, *Chem. Mater.*, **19**, 4396 (2007).
(2) G. Otieno and J. Y. Kim, *J. Ind. Eng. Chem.*, **14**, 187 (2008).
(3) B. W. Cho and M. S. Kim, *J. Ind. Eng. Chem.*, **11**, 594 (2005).
(4) S. E. Bourdo and T. Viswanathan, *Carbon*, **43**, 2983 (2005).
(5) W. P. Wang, C. Y. Pan, and J. S. Wu, *J. Phys. Chem. Solids*, **66**, 1655 (2005).
(6) X. S. Du, M. Xiao, and Y. Z. Meng, *Eur. Polym. J.*, **40**, 1489 (2004).
(7) R. Zhang, Y. Hu, J. Xu, W. Fan, and Z. Chen, *Polym. Degrad. Stabil.*, **85**, 583 (2004).
(8) M. U. Fawn and A. W. Charles, *Polym. Degrad. Stabil.*, **76**, 111 (2002).
(9) H. T. Ham, Y. S. Choi, M. G. Chee, and I. J. Chung, *J. Polym. Sci. Part A: Polym. Chem.*, **44**, 573 (2006).
(10) H. Barraza, F. Pompeo, E. O'Rear, and D. Resasco, *Nano Lett.*, **2**, 797 (2002).
(11) I. Park, M. Kim, H. Lee, and M. S. Lee, *Macromol. Res.*, **15**, 498 (2007).